# Comparison of scattering series solutions for acoustic wave and electromagnetic diffusion equations

Myoung Jae Kwon & Roel Snieder
*Center for Wave Phenomena, Colorado School of Mines*

**ABSTRACT**

Inverse scattering series (ISS) is a tool for the interpretation of geophysical data that theoretically does not require a priori knowledge about the target of an experiment. The ISS method has been applied to seismic exploration, in particular to velocity estimation and multiple suppression. Compared to seismic exploration, electromagnetic methods are characterized by rapid spatial decay of the probing field and strong perturbation of the medium parameters. As a prototype for the convergence of the forward and inverse scattering series, we analyze the 3D Green function for homogeneous media. The analysis suggests that for parameters representing geophysical exploration of hydrocarbon reservoirs, the convergence speed of scattering series solutions for electromagnetic diffusion is faster than that for acoustic wave propagation. The model tests also show that for the diffusion equation, one can improve the convergence of the inverse scattering series by choosing a reference medium that is less conductive than the actual medium is. This research provides insights into the convergence requirements of the ISS method and guidelines for further applications of the ISS method to the interpretation of field data.

**Key words:** inverse scattering series (ISS), acoustic wave equation, electromagnetic diffusion equation

## 1 INTRODUCTION TO SCATTERING SERIES

Scattering theory is a form of perturbation analysis, and the goal of the inverse scattering problem is to obtain a quantitative description of an unknown scatterer from knowledge of the scattering data. The theory originates from inverse problems in quantum scattering theory and formal solutions of inverse scattering problems (Gel'fand & Levitan1951; Jost & Kohn1952; Moses1956; Prosser1969). Inverse scattering series (ISS) describes the model perturbation as a series in order of a scattered field. The ISS method was applied to seismic exploration for reconstruction of subsurface velocity (Weglein *et al.*1981) and attenuation of multiples in seismic reflection data (Weglein *et al.*1997; Weglein *et al.*2003). The main advantage of the ISS method is that no a priori knowledge of the subsurface (e.g., velocity) is assumed and all refraction, diffraction, and multiple reflection phenomena are, in principle, taken into account. Recent studies show that the ISS method can be applied to diverse seismic problems that include imaging, direct non-linear inversion, data reconstruction, and wavefield separation (Ramirez & Weglein2009; Weglein *et al.*2009; Zhang & Weglein2009a; Zhang & Weglein2009b).

Scattering theory relates the difference between the actual (perturbed) and reference (unperturbed) fields to the difference between their corresponding medium properties (Figure 1). We consider the following differential equations as governing equations for the actual and reference media:

$$L(\mathbf{r};\omega)\,G(\mathbf{r},\mathbf{r}_s;\omega) = -\delta(\mathbf{r}-\mathbf{r}_s), \tag{1}$$

$$L_0(\mathbf{r};\omega)\,G_0(\mathbf{r},\mathbf{r}_s;\omega) = -\delta(\mathbf{r}-\mathbf{r}_s), \tag{2}$$

where $L$, $L_0$ and $G$, $G_0$ are the actual and reference differential operators and Green functions, respectively, for a single angular frequency $\omega$, $\delta(\mathbf{r}-\mathbf{r}_s)$ is the Dirac delta function, and $\mathbf{r}$ and $\mathbf{r}_s$ are the receiver and source

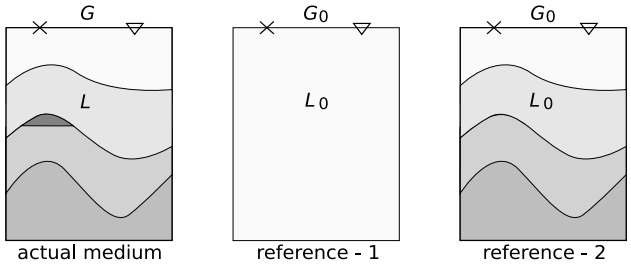


**Figure 1.** Actual medium versus different choices of reference medium. The symbols $\times$ and $\bigtriangledown$ indicate the source and receiver, respectively. $G$ and $G_0$ are the Green functions for the actual and reference media, respectively. Note that given the actual medium, there are several possible choices of the reference medium.

locations, respectively. The information about the actual and reference media properties is encapsulated in $L$ and $L_0$. The perturbation $P$ is defined as the difference between two differential operators:

$$P(\mathbf{r};\omega) = L(\mathbf{r};\omega) - L_0(\mathbf{r};\omega). \tag{3}$$

The Lippmann-Schwinger equation (Taylor1972; Colton & Kress1998) relates $G$, $G_0$ and $P$:

$$G(\mathbf{r},\mathbf{r}_s;\omega) = G_0(\mathbf{r},\mathbf{r}_s;\omega) + \int G_0(\mathbf{r},\mathbf{r}';\omega)P(\mathbf{r}';\omega)G(\mathbf{r}',\mathbf{r}_s;\omega)\,d\mathbf{r}', \tag{4}$$

or in operator form:

$$G = G_0 + G_0PG. \tag{5}$$

The scattered field is the difference between the two Green functions ($G - G_0$) and can be expanded in an infinite series in order of the perturbation $P$ (in operator form):

$$S = G_0PG_0 + G_0PG_0PG_0 + \cdots. \tag{6}$$

Equation (6) is known as the Born, Neumann, or forward scattering series. This series provides an interpretation of the scattered field $S$ in terms of $G_0$ and $P$. The interpretation of the forward scattering series is shown in Figure 2; $G_0PG_0$ denotes the portion of the scattered field $S$ that experiences a single scattering event from points where the actual medium differs from the reference medium; $G_0PG_0PG_0$ denotes the portion that experiences two scattering events, and so on.

The inverse scattering series describes the perturbation $P$ as a series expansion in order of the scattered field $S$:

$$P = P_1 + P_2 + P_3 + \cdots, \tag{7}$$

where $P_n$ is the portion of $P$ that is the $n$th order of the scattered field. Substituting the above equation into equation (6) and equating terms that are equal order of the scattered field $S$, we derive the following set of

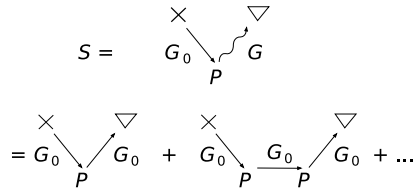


**Figure 2.** Schematic illustration of the forward scattering series from Weglein et al. (2003). The symbols $\times$ and $\bigtriangledown$ indicate source and receiver. $S$, $P$, $G_0$, and $G$ are the scattered field, perturbation, and Green functions for the reference and actual media, respectively. The straight and wiggled arrows indicate signals through the reference and perturbed media, respectively.

integral equations represented in operator form:

$$\begin{aligned}
S &= G_0P_1G_0, && (8)\\
0 &= G_0P_2G_0 + G_0P_1G_0P_1G_0, && (9)\\
0 &= G_0P_3G_0 + G_0P_1G_0P_2G_0 + G_0P_2G_0P_1G_0 \\
&+ G_0P_1G_0P_1G_0P_1G_0, && (10)\\
&\cdots \\
0 &= G_0P_nG_0 + G_0P_1G_0P_{n-1}G_0 + \cdots \\
&+ G_0P_1G_0P_1\cdots P_1G_0P_1G_0. && (11)
\end{aligned}$$

Solving the above set of equations, we determine the perturbation to the $n$th order of the scattered field. Equation (8) is the linear or Born approximation which allows $P_1$ to be determined from the scattered field $S$. $P_2$ is then computed from $P_1$ with equation (9). Equation (10) determines $P_3$ from $P_1$ and $P_2$. Continuing in this manner, the entire series for the perturbation $P$ is constructed, starting with the scattered field. To derive the $n$th order term in the inverse series, we solve the following Fredholm integral equation of the first kind:

$$\begin{aligned}
&f_n(G_0, S, P_1, P_2, \cdots, P_{n-1};\omega) \\
&= \int G_0(\mathbf{r},\mathbf{r}';\omega)P_n(\mathbf{r}';\omega)G_0(\mathbf{r}',\mathbf{r}_s;\omega)\,d\mathbf{r}'. \qquad (12)
\end{aligned}$$

Solving this equation efficiently for $P_n$ is an essential element of application of the inverse scattering series.

In equation (7), we assume that $P_1$ is the portion of $P$ that is linear in the scattered field. In fact, only the linear component in the scattered field ultimately contributes to the reconstruction of the model, and the non-linear components are subtracted in the inversion (Snieder1990a; Snieder1990b). Generally, the series solutions in equations (6) and (7) converge within finite range of perturbation and scattered field (radius of convergence), and the series solutions coincide with the exact solutions inside the radius of convergence. When the series converges, we only require the Green function for the reference medium $G_0$ and the scattered field $S$ for the reconstruction of the perturbation. In other words, we utilize the measured data as it is and do not need a priori knowledge about the actual medium, which

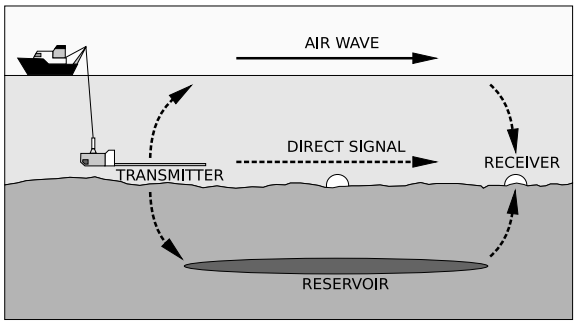


**Figure 3.** Schematic representation of controlled-source electromagnetic (CSEM) exploration from MacGregor et al. (2006). An electromagnetic transmitter is towed close to the seafloor to maximize the coupling of electric and magnetic fields with seafloor rocks. These fields are recorded by receivers deployed on the seafloor some distance from the transmitter.

most geophysical data processing requires. This property of the ISS method demonstrates the potential of the method for geophysical inversion or model reconstruction.

## 2 COMPARISON OF WAVE PROPAGATION AND DIFFUSION IN GEOPHYSICAL EXPLORATION

As existing hydrocarbon reservoirs are being depleted, we are forced to explore hydrocarbon in more challenging environments. Seismic exploration, which is based on wave propagation, provides good structural information of the subsurface medium and has been the major exploration method for the discovery of hydrocarbon reservoirs. Recently, the controlled-source electromagnetic (CSEM) exploration method has been considered a useful complementary tool for hydrocarbon discovery because the method can provide more decisive information about the reservoir composition than the seismic method does. The CSEM method is an electromagnetic exploration method designed for marine environments (Figure 3); the theoretical foundation for the CSEM method was laid in the 1980s (Chave & Cox1982; Cox *et al.*1986). Since then, the application of the CSEM method for hydrocarbon exploration has been extensively studied (Hoversten *et al.*2006; Constable & Srnka2007). The electromagnetic field is sensitive to electric conductivity, which is predominantly influenced by water content within the subsurface: increasing water content causes larger conductivity. Hydrocarbons, whether gas or petroleum, are poor electric conductors. The significant difference of electric conductivity in water and hydrocarbon makes the CSEM method an ideal tool for distinguishing a hydrocarbon reservoir from a water saturated reservoir.

Assuming time harmonic dependency ($e^{-i\omega t}$) and a given electric current source $\mathbf{J}^s$, the electric field $\mathbf{E}$ and magnetic field $\mathbf{H}$ responses within an isotropic medium are derived from the following frequency domain expressions of Maxwell's equations (Jackson1999):

$$\nabla \times \mathbf{E}(\mathbf{r}) - i\omega\mu(\mathbf{r})\mathbf{H}(\mathbf{r}) = 0, \tag{13}$$

$$\nabla \times \mathbf{H}(\mathbf{r}) - [\sigma(\mathbf{r}) - i\omega\epsilon(\mathbf{r})]\,\mathbf{E}(\mathbf{r}) = \mathbf{J}^s(\mathbf{r}), \tag{14}$$

where $\mu$, $\sigma$ and $\epsilon$ are magnetic permeability, electric conductivity and dielectric permittivity of the medium, respectively. The electric and magnetic fields can be expressed in terms of vector potential $\mathbf{A}$ as

$$\mathbf{E}(\mathbf{r}) = i\omega\mu\mathbf{A}(\mathbf{r}) + \frac{\nabla(\nabla \cdot \mathbf{A}(\mathbf{r}))}{\sigma - i\omega\epsilon}, \tag{15}$$

$$\mathbf{H}(\mathbf{r}) = \nabla \times \mathbf{A}(\mathbf{r}). \tag{16}$$

Within a homogeneous medium, equations (13) and (14) yield the following Helmholtz equation of vector potential:

$$\nabla^2\mathbf{A}(\mathbf{r}) + \left(\omega^2\mu\epsilon + i\omega\mu\sigma\right)\mathbf{A}(\mathbf{r}) = -\mathbf{J}^s(\mathbf{r}), \tag{17}$$

where the two terms, $\mu\epsilon$ and $\mu\sigma$, are related to the wave velocity $c$ and diffusivity $d$ of the response:

$$\mu\epsilon = \frac{1}{c^2} \quad \text{and} \quad \mu\sigma = \frac{1}{d}. \tag{18}$$

In many geophysical applications, the magnetic permeability can be assumed to be that of free space.

In geophysical applications of electromagnetic methods, wave propagation is significant in the high frequency range (i.e., ground penetrating radar) or in an insulating medium (i.e., air). For most earth materials and frequencies of electromagnetic methods used in hydrocarbon exploration, diffusion is dominant and the contribution of wave propagation is negligible. In contrast, seismic exploration is always governed by wave propagation. Seismic exploration is performed over a scale of many wavelengths, whereas the CSEM signal exhibits strong spatial decay and diffuses over a few skin depths $\delta$ that describe the length scale where the amplitude decays to $e^{-1}$. Furthermore, the strength of the medium perturbation in CSEM exploration is stronger than that in seismic exploration. In other words, the range of electric conductivity in the earth medium is generally wider than the range of seismic wave velocity (Palacky1987; Mavko *et al.*1998).

The application of the ISS method to geophysical exploration has focused on seismic exploration (Weglein *et al.*1981; Weglein *et al.*1997; Weglein *et al.*2003). In this study, we perform a comparative analysis of scattering series methods for acoustic wave and electromagnetic diffusion equations and study the feasibility of applying the ISS method to electromagnetic exploration, which involves a diffusive field within a strongly perturbed medium.

## 3 FORMULATION OF SCATTERING SERIES SOLUTIONS

For the identification of the differences of the properties of the scattering series method for the acoustic wave and electromagnetic diffusion equations, we consider the simplest case of a homogeneous 3D medium and compare two different states of this infinite homogeneous medium. We analyze the series expression between the perturbation and scattered field at a single point and study the spatial variation of the series expansion.

We consider hydrocarbon exploration and assume that wave propagation of the electromagnetic response is negligible within the medium. We derive the electromagnetic response from equations (15) - (17). Equation (17) is the Helmholtz equation of vector potential $\mathbf{A}$, and each component of the vector potential is proportional to the corresponding component of the electric current source $\mathbf{J}_s$. We can therefore describe the electromagnetic diffusion by the Helmholtz equation of a scalar field. The acoustic wave propagation also involves a scalar field, i.e., pressure field. Given a point source at the origin, both the acoustic wave propagation and electromagnetic diffusion within the homogeneous medium are described by the Helmholtz equation of the scalar Green function $G$:

$$\nabla^2 G(\mathbf{r}) + k^2 G(\mathbf{r}) = -\delta(\mathbf{r}), \tag{19}$$

where wavenumber $k$ is given by

$$k^2 = \begin{cases} \omega^2/c^2 \text{ (acoustic wave equation)}, \\ i\omega\mu\sigma \text{ (electromagnetic diffusion equation)}. \end{cases} \tag{20}$$

In this study, we assume that the magnetic permeability $\mu$ is that of free space and that acoustic wave velocity $c$ and electric conductivity $\sigma$ are real, which implies that wavenumber $k$ is real for the wave equation and complex for the diffusion equation. The 3D Green function for the Helmholtz equation is given as (Morse & Feshbach1953)

$$G(\mathbf{r}) = \frac{1}{4\pi r} e^{ikr}, \tag{21}$$

where $r = |\mathbf{r}|$.

We denote wavenumbers of the reference and perturbed media as $k_0$ and $k$, respectively. From equation (3), the perturbation is defined as

$$P = k^2 - k_0^2, \tag{22}$$

and wavenumber of the perturbed medium is expressed as

$$k = k_0 \sqrt{1 + \frac{P}{k_0^2}}. \tag{23}$$

The scattered field $S(\mathbf{r})$ is the difference between the Green functions of the perturbed and reference media:

$$S(\mathbf{r}) = \frac{1}{4\pi r} \left[ \exp\left( ik_0 r \sqrt{1 + \frac{P}{k_0^2}} \right) - \exp\left(ik_0 r\right) \right], \tag{24}$$

and the forward scattering series expresses the scattered field $S(\mathbf{r})$ as a series in order of the perturbation $P$. Note that a function of a complex variable $z$, $f(z) = \sqrt{1+z}$, has a singular point (branch point) at $z = -1$, and the radius of convergence of the Taylor series expansion around $z = 0$ extends up to the singular point. The series for the exponential is absolutely convergent. Therefore, equation (24) shows that the forward scattering series converges only for small perturbations compared to the reference medium properties such that

$$\left| \frac{P}{k_0^2} \right| < 1. \tag{25}$$

The above requirement of convergence implies the following convergence criteria:

$$\begin{cases} c > c_0/\sqrt{2} \text{ (acoustic wave equation)}, \\ \sigma < 2\,\sigma_0 \quad \text{(electromagnetic diffusion equation)}. \end{cases} \tag{26}$$

Taylor series expansion on equation (24) shows that the $n$th order term in the forward series is expressed as

$$S_n(\mathbf{r}) = G_0(\mathbf{r})\, \alpha_n(ik_0 r) \left[ \frac{P}{k_0^2} \right]^n, \tag{27}$$

where $\alpha_n(ik_0 r)$ is $n$th order power series of $ik_0 r$ such that

$$\alpha_n(ik_0 r) = \frac{1}{2^n\, n!} \sum_{m=1}^{n} \beta_{n,m}\, (ik_0 r)^{n-m+1}, \tag{28}$$

and

$$\beta_{n,m} = \begin{cases} 1 & (m = 1), \\ -\dfrac{\beta_{n,m-1}}{m-1} \displaystyle\sum_{l=m-1}^{n-1} l & (m = 2, 3, 4, \cdots, n). \end{cases} \tag{29}$$

The convergence rate is, therefore,

$$R_n^F(\mathbf{r}) = \left| \frac{S_{n+1}(\mathbf{r})}{S_n(\mathbf{r})} \right| = \left| \frac{\alpha_{n+1}(ik_0 r)}{\alpha_n(ik_0 r)} \right| \left| \frac{P}{k_0^2} \right|. \tag{30}$$

The above equation shows that $R_n^F$ is proportional to $|P/k_0^2|$, and the forward scattering series converges fast for weak perturbation. To appreciate the contribution of $\alpha_{n+1}/\alpha_n$ on the convergence rate, we consider an acoustic wave problem where the frequency $f$ is 50 Hz, wave velocity $c$ is 3,000 m/s, and wavenumber $k_0$ is about 0.1 $\mathrm{m}^{-1}$. Figure 4 shows the variation of $|\alpha_{n+1}/\alpha_n|$ at two spatial locations: one is 3 wavelengths apart from the source ($k_0 r = 6\pi$) and the other is 6 wavelengths ($k_0 r = 12\pi$). The figure shows that $|\alpha_{n+1}/\alpha_n|$ is larger for $k_0 r = 12\pi$ than for $k_0 r = 6\pi$ and implies that as the source-receiver offset increases, more series terms are necessary to reach convergence.

The formal expression of convergence rate given in equation (30) is valid for both the wave and diffusion equations. The wavenumber of the diffusion problem (equation (20)) has real and imaginary parts, and the

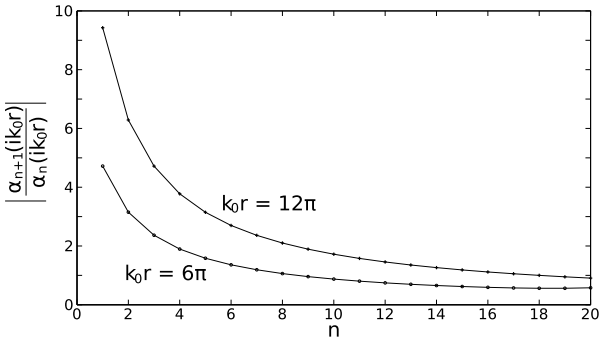


**Figure 4.** Convergence rate of forward scattering series. The ratio $|\alpha_{n+1}/\alpha_n|$ in equation (30) for increasing number of $n$ is compared at two spatial locations: one is 3 wavelengths apart from the source ($k_0r = 6\pi$) and the other is 6 wavelengths ($k_0r = 12\pi$).

Green function for the diffusion equation generally exhibits faster spatial decay than that for the wave equation, which has real wavenumber. However, equation (30) indicates that there is no fundamental difference in the convergence rate between the forward scattering series for the diffusion equation and the series for the wave equation. In fact, fast spatial decay of the diffusive field does not necessarily mean fast convergence of the scattering series for the diffusion equation. This counterintuitive behavior of the convergence rate can be comprehended by considering the following three functions: $e^x$, $e^{-x}$, and $e^{ix}$. The three functions exhibit different variations as a function of $x$, but their Taylor series expansions in the variable $x$ show the same convergence rate. This property of the convergence rate implies that the comparison of the convergence speed between wave propagation and diffusion depends on the specific parameters that we incorporate instead of the difference in the behavior of the physical fields. In the following, we choose representative parameters that reflect the hydrocarbon exploration situations and compare the convergence of the forward scattering series for the acoustic wave equation with that for the electromagnetic diffusion equation. The details of the parameters are introduced in the next section.

While the forward scattering series expresses the scattered field $S(\mathbf{r})$ as a power series in order of the perturbation $P$, the inverse series expresses the perturbation as a power series in order of the scattered field. Rewriting equation (24), the perturbation is expressed as a function of the scattered field:

$$P(\mathbf{r}) = -\frac{2ik_0}{r}\ln\left(1+\frac{S(\mathbf{r})}{G_0(\mathbf{r})}\right) - \frac{1}{r^2}\left[\ln\left(1+\frac{S(\mathbf{r})}{G_0(\mathbf{r})}\right)\right]^2. \quad (31)$$

Note that the function $f(z) = \ln(1+z)$ is singular at $z = -1$, and the radius of convergence of the Taylor series expansion centered at $z = 0$ extends up to the singular point. Equation (31) therefore shows that the inverse scattering series converges only for weak scattered fields that satisfy

$$\left|\frac{S(\mathbf{r})}{G_0(\mathbf{r})}\right| = \left|\frac{G(\mathbf{r})}{G_0(\mathbf{r})} - 1\right| = \left|e^{i(k-k_0)r} - 1\right| < 1. \quad (32)$$

By performing a Taylor series expansion of equation (31), it can be shown that the $n$th order term in the inverse series is given by

$$P_n(\mathbf{r}) = 2\left[\gamma_n(k_0, r) + \zeta_n(r)\right]\left[\frac{S(\mathbf{r})}{G_0(\mathbf{r})}\right]^n, \quad (33)$$

where

$$\gamma_n(k_0, r) = (-1)^n \frac{ik_0}{nr}, \quad (34)$$

$$\zeta_n(r) = \frac{\eta_n}{n!\, r^2}, \quad (35)$$

and

$$\eta_n = \begin{cases} 0 & (n = 1), \\ -(n-1)\eta_{n-1} + (-1)^{n-1}(n-2)! & (n = 2, 3, 4, \cdots). \end{cases} \quad (36)$$

The above formal expression of the inverse scattering series is valid for both the wave and diffusion equations. Figure 5 shows the absolute values of $\gamma_n$ and $\zeta_n$ in equation (33). When the wavenumber of the reference medium is $k_0 = 0.1$ m$^{-1}$, $|\zeta_n|$ is much smaller than $|\gamma_n|$ at $r = 100$ m. The coefficient $|\gamma_n|$ is proportional to $k_0/r$ and $|\zeta_n|$ is to $1/r^2$. Therefore, compared to $\zeta_n$, $\gamma_n$ is significant at a large source-receiver offset and for a large wavenumber of the reference medium. Ignoring $\zeta_n$, the convergence rate of the inverse scattering series is approximated as

$$R_n^I = \left|\frac{P_{n+1}(\mathbf{r})}{P_n(\mathbf{r})}\right| \simeq \left|\frac{\gamma_{n+1}}{\gamma_n}\frac{S(\mathbf{r})}{G_0(\mathbf{r})}\right| = \left|\frac{n}{n+1}\frac{S(\mathbf{r})}{G_0(\mathbf{r})}\right|. \quad (37)$$

The above equation shows that as the scattering becomes stronger, the convergence speed of the inverse scattering series becomes slower.

## 4 MODEL TESTS OF SCATTERING SERIES SOLUTIONS

As noted in the previous section, a comparison of the convergence rates between wave propagation and diffusion depends on the specific parameters that we incorporate. We therefore choose parameters that are widely applied for exploring hydrocarbon reservoirs. For the application of the scattering series expressions (given by equations (27) and (33)) to the acoustic wave and electromagnetic diffusion problems, we adopt the parameters summarized in Table 1. Note we assume a velocity perturbation of 10% for the acoustic wave problem and a perturbation with a factor 10 ($\sigma_0/\sigma = 10$) for the electromagnetic diffusion problem. We also assume that magnetic permeability of the medium is the same as that of free space ($\mu = 4\pi \times 10^{-7}$ N/A$^2$).

**Table 1.** Summary of physical parameters adopted for model tests, where $c$ and $\sigma$ represent acoustic wave velocity and electric conductivity, respectively. Wavenumber $k$ is derived from equation (20). The perturbation is real for the acoustic wave problem and imaginary for the electromagnetic diffusion problem.

| Acoustic wave problem | | Electromagnetic diffusion problem | |
|---|---|---|---|
| $f$ | 50 Hz | $f$ | 10 Hz |
| $c_0$ | $3.0 \times 10^3$ m/s | $\sigma_0$ | $1.0 \times 10^{-1}$ S/m |
| $c$ | $3.3 \times 10^3$ m/s | $\sigma$ | $1.0 \times 10^{-2}$ S/m |
| $k_0^2$ | $1.10 \times 10^{-2}$ m$^{-2}$ | $\lvert k_0^2 \rvert$ | $7.90 \times 10^{-6}$ m$^{-2}$ |
| $k^2$ | $0.91 \times 10^{-2}$ m$^{-2}$ | $\lvert k^2 \rvert$ | $0.79 \times 10^{-6}$ m$^{-2}$ |
| $P = k^2 - k_0^2$ | $-0.19 \times 10^{-2}$ m$^{-2}$ | $\lvert P \rvert = \lvert k^2 - k_0^2 \rvert$ | $7.11 \times 10^{-6}$ m$^{-2}$ |

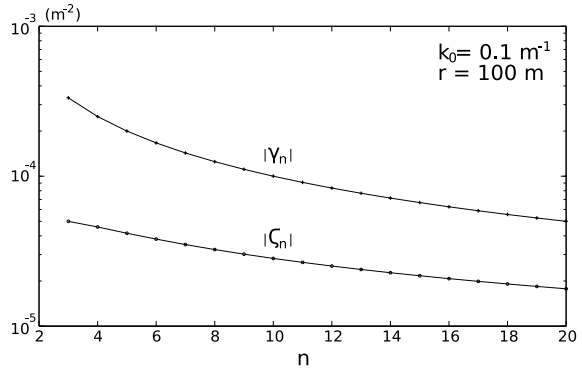


**Figure 5.** Comparison of the absolute values of $\gamma_n$ and $\zeta_n$ in equation (33). For $k_0 = 0.1$ m$^{-1}$ and $r = 100$ m, $|\zeta_n|$ is much smaller than $|\gamma_n|$. The two terms are dependent on $k_0/r$ and $1/r^2$, respectively, which implies $\gamma_n$ is significant at a large source-receiver offset and for a large wavenumber of the reference medium.

Figures 6 and 7 show the spatial variation of the forward scattering series for the acoustic wave and electromagnetic diffusion equations, respectively. The solutions derived from the forward series (solid curve) are compared with the analytic solution of the scattered field (dotted curve), which is expressed as

$$S(\mathbf{r}) = \frac{e^{ikr} - e^{ik_0 r}}{4\pi r}. \tag{38}$$

The scattered field of the acoustic wave equation (dotted curve in Figure 6) exhibits spatial oscillations, amplitude modulation, and geometric spreading. The scattered field of the electromagnetic diffusion equation (dotted curve in Figure 7) shows exponential amplitude decay and monotonous phase change. From equation (27), the first order term in the forward series is

$$S_1(\mathbf{r}) = \frac{iP}{8\pi k_0} e^{ik_0 r} \tag{39}$$

and near the source, exhibits better agreement with the analytic solution than at the far receiver location. As we include higher order terms, the partial sum of the forward series approaches the analytical solution of the scattered field. Note that except for short source-receiver offset, the forward scattering series for the electromagnetic diffusion equation ($N = 5$ in the middle panel of Figure 7) requires fewer terms to achieve good agreement with the analytic solution than the series for the acoustic wave equation ($N = 15$ in the middle panel of Figure 6). We therefore conclude that for the employed parameters (Table 1) which are representative of hydrocarbon exploration, the forward scattering series for the electromagnetic diffusion equation converges

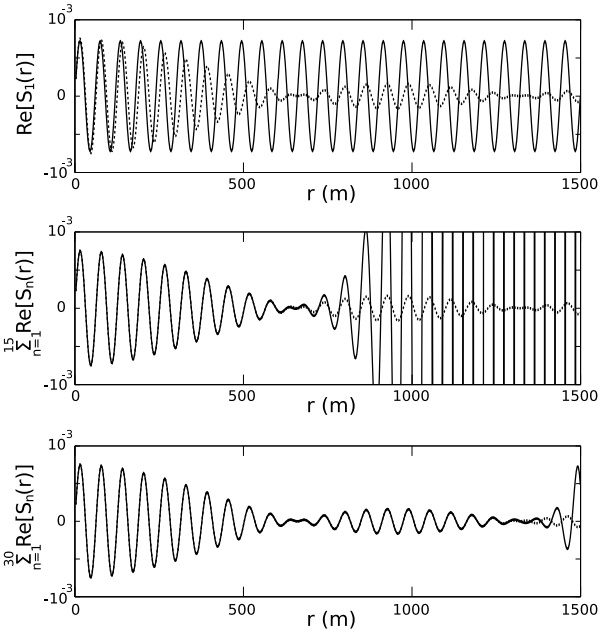


**Figure 6.** Spatial variation of forward scattering series for the acoustic wave equation (real part only). The employed parameters are summarized in Table 1. The solutions derived from the forward series (solid curve) are compared with the analytic solution of the scattered field (dotted curve). The top, middle, and bottom panels show the partial sum $\sum_{n=1}^{N} S_n(\mathbf{r})$ for $N = 1$, $N = 15$, and $N = 30$, respectively. As we include higher order terms in the forward series, the partial sum of the forward series approaches the analytic solution of the scattered field at an increasing range of $r$.

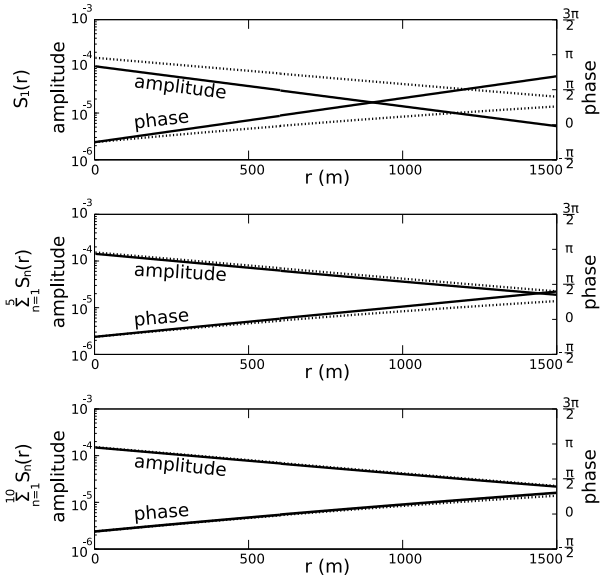


**Figure 7.** Spatial variation of the forward scattering series for the electromagnetic diffusion equation. The employed parameters are summarized in Table 1. The solutions derived from the forward series (solid curve) are compared with the analytic solution of the scattered field (dotted curve). The top, middle, and bottom panels show the partial sum $\sum_{n=1}^{N} S_n(\mathbf{r})$ for $N = 1$, $N = 5$, and $N = 10$, respectively. As we include higher order terms in the forward series, the partial sum of the forward series approaches the analytic solution of the scattered field at an increasing range of $r$.

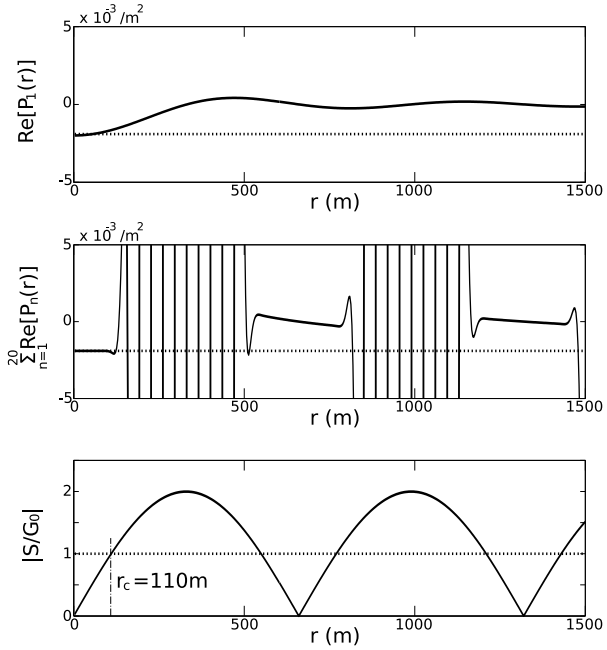


**Figure 8.** Spatial variation of the inverse scattering series for the acoustic wave equation (real part only). The employed parameters are summarized in Table 1. In the top and middle panels, the solutions derived from the inverse series (solid curve) are compared with the exact value of the perturbation $\omega^2(1/c^2 - 1/c_0^2)$ (dotted line) which is real. The first term in the inverse series (the top panel) exhibits significant discrepancy from the exact value. The partial sum up to the 20th order term in the inverse series (the middle panel) converges to the exact value within a limited range where $r < r_c$ and diverges elsewhere. The bottom panel shows the spatial variation of $|S(\mathbf{r})/G_0(\mathbf{r})|$.

faster and requires fewer series terms than does the series for the acoustic wave equation.

Figures 8 and 9 show the spatial variation of the inverse scattering series for the acoustic wave and electromagnetic diffusion equations, respectively. The solutions derived from the inverse series (solid curve) are compared with the exact value of the perturbation (dotted line) which is real for the wave equation and imaginary for the diffusion equation. In these figures, $r_c$ describes the maximum distance for which the inverse scattering series converges as described below. Considering the convergence criterion given in equation (32), the variation of $|S/G_0|$ (solid curve) is also compared with the threshold value for convergence (dotted line). The first order term in the inverse series exhibits significant deviation from the exact value. The partial sum of the inverse series up to the 20th order term converges to the exact value within the range that extends from $r = 0$ to the location where the convergence criterion is satisfied. However, the partial sum of the inverse series diverges for $r > r_c$. Compared to the inverse series for the acoustic wave equation (Figure 8), the series for the electromagnetic diffusion equation (Figure 9) converges to the exact value of the perturbation in a wider spatial range. This convergence pattern suggests that for the employed parameters, the inverse scattering series for the electromagnetic diffusion equation converges faster than does the series for the acoustic wave equation. The above observations also reveal that the convergence criterion given in equation (32) plays a crucial role in the reconstruction of the perturbation. We therefore perform more detailed analysis on the convergence criterion.

As noted before, wavenumber $k$ is real for the acoustic wave equation. Denoting the spatial radius of convergence for the inverse series of the wave equation as $r_c$, we derive the following relation from equation (32):

$$\left| e^{i(k-k_0)r_c} - 1 \right| = 1. \tag{40}$$

The spatial radius of convergence is, therefore, given as

$$r_c = \frac{\pi}{3\,|k - k_0|}. \tag{41}$$

In case of the electromagnetic diffusion problem, the wavenumber is derived from $k^2 = i\omega\mu\sigma$, and we denote the wavenumber as

$$k = \frac{1+i}{\sqrt{2}}|k|. \tag{42}$$

The convergence criterion given in equation (32) is

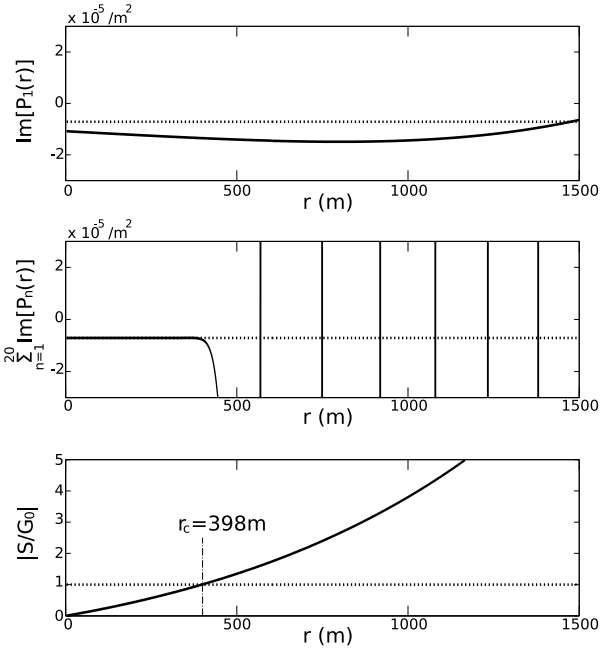


**Figure 9.** Spatial variation of the inverse scattering series for the electromagnetic diffusion equation (imaginary part only). The employed parameters are summarized in Table 1. In the top and middle panels, the solutions derived from the inverse series (solid curve) are compared with the exact value of the perturbation $i\omega\mu(\sigma - \sigma_0)$ (dotted line) which is imaginary. The first term in the inverse series (the top panel) exhibits significant discrepancy from the exact value. The partial sum up to the 20th order term in the inverse series (the middle panel) converges to the exact value within a limited range where $r < r_c$ and diverges elsewhere. The bottom panel shows the spatial variation of $|S(\mathbf{r})/G_0(\mathbf{r})|$.

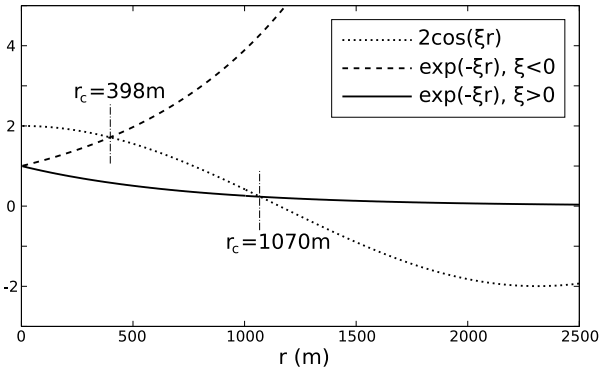


**Figure 10.** Derivation of the spatial radius of convergence $r_c$ for the electromagnetic diffusion problem. The dashed and solid curves show the left-hand side of equation (45) for $\xi < 0$ and $\xi > 0$, respectively, while the dotted curve shows the right-hand side of equation (45). Applying the parameters summarized in Table 1, $r_c$ is derived as 398 m. On the other hand, by switching the two conductivity values in Table 1 ($\sigma \leftrightarrow \sigma_0$), $r_c$ is derived as 1070 m.

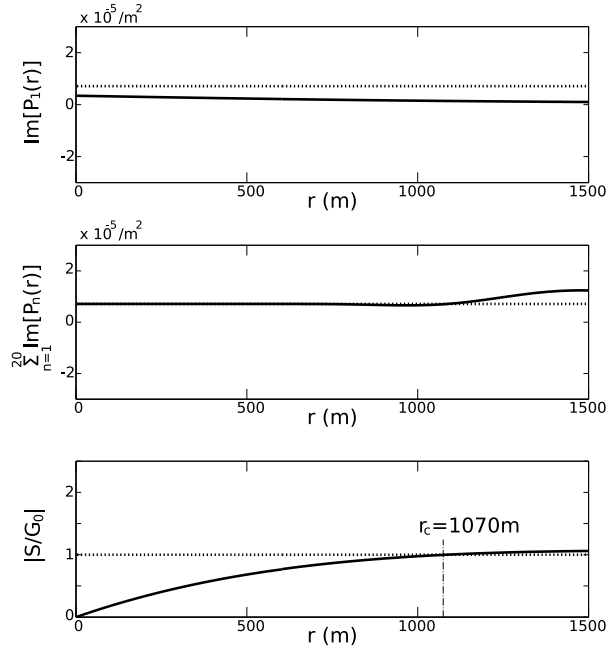


**Figure 11.** Spatial variation of the inverse scattering series for the electromagnetic diffusion equation (imaginary part only). The medium properties of the perturbed and reference media are switched from the previous case shown in Figure 9 and Table 1. Note that the spatial range where $|S(\mathbf{r})/G_0(\mathbf{r})| < 1$ is wider than the case shown in Figure 9.

rewritten as follows:

$$\left|\frac{S(\mathbf{r})}{G_0(\mathbf{r})}\right| = \left|e^{-\frac{|k|-|k_0|}{\sqrt{2}}r} e^{i\frac{|k|-|k_0|}{\sqrt{2}}r} - 1\right| < 1. \qquad (43)$$

Denoting $\xi = (|k| - |k_0|)/\sqrt{2}$, we establish the following relation at $r = r_c$ (the spatial radius of convergence for the inverse series of the diffusion equation):

$$\left|e^{-\xi r} e^{i\xi r} - 1\right| = 1, \qquad (44)$$

which can be simplified as

$$e^{-\xi r} = 2\cos\xi r. \qquad (45)$$

Equation (45) is a transcendental equation for the spatial radius of convergence $r_c$ that is analyzed graphically in Figure 10. The dotted curve shows the right-hand side of equation (45) while the dashed and solid curves show the left-hand side for $\xi < 0$ and $\xi > 0$, respectively. The distance $r_c$ for which the inverse scattering series converges is larger for positive value of $\xi$ ($\sigma > \sigma_0$) than for negative value of $\xi$ ($\sigma < \sigma_0$). This means that the spatial radius of convergence is larger when choosing a reference model with a small electric conductivity.

Equation (43) shows that as $r$ increases, the ratio $|S/G_0|$ exhibits exponential variation with distance: there is exponential decrease when $|k| > |k_0|$ ($\sigma > \sigma_0$) and exponential growth when $|k| < |k_0|$ ($\sigma < \sigma_0$). The inverse scattering problem aims to recover the unknown

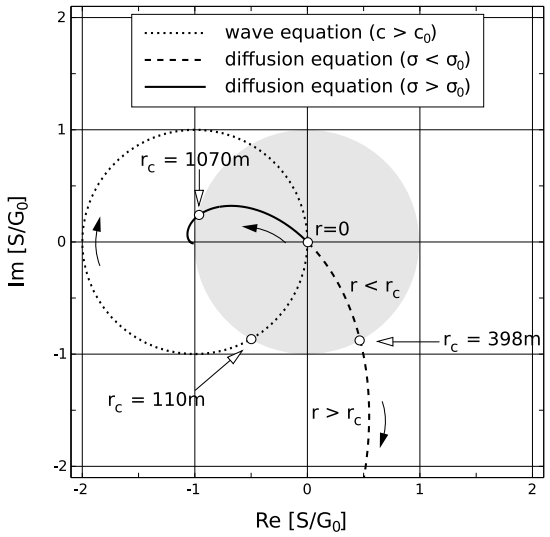


**Figure 12.** The variation of $S/G_0$ in the complex plane for different values of $r$. The origin of the complex plane indicate $r = 0$, and the arrows denote the directions of increasing $r$. Three different cases shown in Figures 8, 9, and 11 are compared. The shaded region denotes the area where the inverse series converges.

perturbation from the measured field and a reference model, and we have freedom of choosing a reference model. Therefore, the exponential variation of the ratio $|S/G_0|$ in equation (43) illustrates that given the actual medium, we can accelerate the convergence of the inverse series for the electromagnetic diffusion equation by choosing a reference medium that is less conductive (smaller wavenumber) than the actual medium. On the other hand, the acoustic wave equation has a real wavenumber, and the sign of $k - k_0$ is irrelevant to the convergence criterion (equation (41)). Figure 11 shows the spatial variation of the inverse scattering series for the electromagnetic diffusion equation when the perturbed and reference media switch roles ($\sigma \leftrightarrow \sigma_0$) from the previous case shown in Figure 9. Compared to the case when the reference medium is more conductive than the actual medium (Figure 9), the spatial range of the convergence shown in Figure 11 is wider.

Figure 12 shows the path of $S/G_0$ in the complex plane as the source-receiver offset $r$ increases for three different cases: the inverse scattering series for the acoustic wave equation (dotted curve), the series for the electromagnetic diffusion equation that corresponds to Figure 9 (dashed curve), and the series for the electromagnetic diffusion equation with the reversed medium properties (solid curve). As the source-receiver distance increases, the value of $S/G_0$ moves away from the origin. In the case of acoustic wave propagation, the path forms a closed circle, and the sign of $c - c_0$ determines the direction of the movement as $r$ increases (clockwise direction when $c > c_0$ and counterclockwise direction when $c < c_0$). On the other hand, the path of $S/G_0$ does not form a closed circle for the electromagnetic diffusion problem. Depending on the sign of $\sigma - \sigma_0$, the ratio $S/G_0$ moves out of the convergence area ($\sigma < \sigma_0$) or converges to the point where $S/G_0 = -1$ ($\sigma > \sigma_0$). This shows that the convergence of the inverse series for the electromagnetic diffusion equation can be facilitated by choosing a reference medium that is less conductive than the actual medium. The different paths represented by the dashed curve ($\sigma < \sigma_0$) and solid curve ($\sigma > \sigma_0$) demonstrates the significance of the choice of the reference medium for the convergence of the inverse scattering series for the electromagnetic diffusion problem.

## 5 CONCLUSIONS

We analyzed the difference between applying the scattering series method to the acoustic wave and electromagnetic diffusion equations for an infinite 3D medium. Analysis of the formal expressions of the scattering series solutions shows that there is no fundamental difference in the convergence rate between the forward scattering series for the acoustic wave equation and the series for the electromagnetic diffusion equation; the analysis also illustrates that rapid spatial decay of the diffusive field does not necessarily mean fast convergence of the scattering series for the diffusion equation. The model tests suggest, however, that for parameters representing geophysical experiments, the convergence speed of the scattering series solutions for the electromagnetic diffusion equation is faster than that for the acoustic wave equation. The model tests also show that for the electromagnetic diffusion equation, we can facilitate the convergence of the inverse scattering series by designing a reference medium that is less conductive than the actual medium. In this study, we considered homogeneous media where the electromagnetic signal diffuses away from the source, and there is no signal that diffuses back from any perturbed structure, which we eventually aim to reconstruct. It requires further research to identify how much we can generalize the above conclusions to the inverse scattering series problems of a 2D or 3D model reconstruction.

## 6 ACKNOWLEDGEMENTS

This work was supported by the Consortium Project on Seismic Inverse Methods for Complex Structures at Center for Wave Phenomena (CWP). We acknowledge Arthur Weglein (University of Houston), Evert Slob (Delft University of Technology) and Yuanzhong Fan for helpful information, discussions, and suggestions. We are also grateful to colleagues of CWP for valuable discussions and technical help.

## REFERENCES


Chave, A., and Cox, C. S., 1982, Controlled electromagnetic sources for measuring electrical conductivity beneath the oceans 1. forward problem and model study: Journal of Geophysical Research, **87**, no. B7, 5327 – 5338.

Colton, D., and Kress, R., 1998, Inverse acoustic and electromagnetic scattering theory: , Springer, 2nd edition.

Constable, S., and Srnka, L., 2007, An introduction to marine controlled-source electromagnetic methods for hydrocarbon exploration: Geophysics, **72**, no. 2, WA3 – WA12.

Cox, C. S., Constable, S. C., Chave, A. D., and Webb, S. C., 1986, Controlled-source electromagnetic sounding of the oceanic lithosphere: Nature, **320**, no. 6057, 52 – 54.

Gel'fand, I. M., and Levitan, B. M., 1951, On the determination of a differential equation from its spectral function: Izvestiya Akademii Nauk SSSR Seriya Matematicheskaya, **15**, no. 4, 309 – 360.

Hoversten, G. M., Cassassuce, F., Gasperikova, E., Newman, G. A., Chen, J., Rubin, Y., Hou, Z., and Vasco, D., 2006, Direct reservoir parameter estimation using joint inversion of marine seismic AVA and CSEM data: Geophysics, **71**, no. 3, C1 – C13.

Jackson, J. D., 1999, Classical electrodynamics: , John Wiley & Sons, 3rd edition.

Jost, R., and Kohn, W., 1952, Construction of a potential from a phase shift: Physical Review, **87**, no. 6, 977 – 992.

Mavko, G., Mukerji, T., and Dvorkin, J., 1998, The rock physics handbook - tools for seismic analysis in porous media: , Cambridge University Press.

Morse, P. M., and Feshbach, H., 1953, Methods of theoretical physics: , McGraw Hill Company.

Moses, H. E., 1956, Calculation of the scattering potential from reflection coefficients: Physical Review, **102**, no. 2, 559 – 567.

Palacky, G. J., 1987, Resistivity characteristics of geologic targets: Resistivity characteristics of geologic targets:, 53 – 129.

Prosser, R. T., 1969, Formal solutions of inverse scattering problems: Journal of Mathematical Physics, **10**, no. 10, 1819 – 1822.

Ramirez, A. C., and Weglein, A. B., 2009, Green's theorem as a comprehensive framework for data reconstruction, regularization, wavefield separation, seismic interferometry and wavelet estimation: A tutorial: Geophysics, **74**, no. 6, W35 – W62.

Snieder, R., 1990a, A perturbative analysis of non-linear inversion: Geophysical Journal International, **101**, no. 3, 545 – 556.

——— 1990b, The role of the born approximation in nonlinear inversion: Inverse Problems, **6**, no. 2, 247 – 266.

Taylor, J. R., 1972, Scattering theory - the quantum theory of nonrelativistic collisions: , Wiley.

Weglein, A. B., Boyse, W. E., and Anderson, J. E., 1981, Obtaining three-dimensional velocity information directly from reflection seismic data: An inverse scattering formalism: Geophysics, **46**, no. 8, 1116 – 1120.

Weglein, A. B., Gasparotto, F. A., Carvalho, P. M., and Stolt, R. H., 1997, An inverse-scattering series method for attenuating multiples in seismic reflection data: Geophysics, **62**, no. 6, 1975 – 1989.

Weglein, A. B., Araujo, F. V., Carvalho, P. M., Stolt, R. H., Matson, K. H., Coates, R. T., Corrigan, D., Foster, D. J., Shaw, S. A., and Zhang, H., 2003, Inverse scattering series and seismic exploration: Inverse Problems, **19**, no. 6, R27 – R83.

Weglein, A. B., Zhang, H., Ramirez, A. C., Liu, F., and Lira, J. E. M., 2009, Clarifying the underlying and fundamental meaning of the approximate linear inversion of seismic data: Geophysics, **74**, no. 6, WCD1 – WCD13.

Zhang, H., and Weglein, A. B., 2009a, Direct non-linear inversion of multi-parameter 1D elastic media using the inverse scattering series: Geophysics, **74**, no. 6, WCD15 – WCD27.

——— 2009b, Direct nonlinear inversion of 1D acoustic media using inverse scattering subseries: Geophysics, **74**, no. 6, WCD29 – WCD39.